The pseudogap and photoemission spectra in the attractive Hubbard model

1999 J. Phys.: Condens. Matter 11 741

(http://iopscience.iop.org/0953-8984/11/3/013)

J. Phys.: Condens. Matter **11** (1999) 741–748. Printed in the UK PII: S0953-8984(99)96731-0

The pseudogap and photoemission spectra in the attractive Hubbard model

P E Kornilovitch† and Bumsoo Kyung‡§

† Blackett Laboratory, Imperial College, Prince Consort Road, London SW7 2BZ, UK
‡ Max-Planck-Institut für Physik komplexer Systeme, Nöthnitzer Strasse 38, D-01187, Dresden, Germany

Received 12 August 1998

Abstract. Angle-resolved photoemission spectra are calculated microscopically for the two-dimensional attractive Hubbard model. A system of self-consistent T-matrix equations are solved numerically in the real-time domain. The single-particle spectral function has a two-peak structure resulting from the presence of bound states. The spectral function is suppressed at the chemical potential, leading to a pseudogap-like behaviour. At high temperatures and densities the pseudogap diminishes and finally disappears; these findings are similar to the experimental observations for the cuprates.

Real-space pairing [1] is the simplest physical idea that enables one to explain the pseudogap phenomenon observed for the normal state of high-T_c superconductors (HTSC) [2–13]. At low temperatures and densities, carriers are paired in weakly overlapping bound states separated from the single-particle band by a binding energy of the order of a few hundred degrees. The chemical potential is located between the two bands, thereby reducing the intensity of the low-energy single-particle (photoemission, specific heat, tunnelling), spin (susceptibility, nuclear relaxation rate), and particle–hole (optical conductivity) processes. At temperatures of the order of the binding energy, carriers become unbound and restore the Fermi-liquid behaviour. The layered structure of the cuprates supports this scenario, since reduced dimensionality favours pairing. Also, the phenomenology of a charged Bose gas can be quite successfully used in the explanation of a number of normal and superconducting properties of HTSC [1, 14, 15].

It is therefore important to study model systems with pairing, such as the two-dimensional attractive Hubbard model. The simplicity of the model allows one to separate the net effect of the attractive interaction from the complications related to the origin of the pairing mechanism and to the complicated dependence of the effective potential on microscopic parameters. One successful application of the attractive Hubbard model to the physics of cuprates is due to Randeria and co-workers [16, 17]. Using the quantum Monte Carlo method, they found a significant reduction of the static spin susceptibility and nuclear relaxation rate at low temperatures and intermediate couplings. Recently, Vilk *et al* [18] found a pseudogap in the spectral function of the attractive Hubbard model using Monte Carlo simulations and the maximum-entropy technique. Thus, it was demonstrated that real-space pairing can account for some unusual properties of HTSC.

§ Present address: Department of Physics, University of Sherbrooke, Sherbrooke, Quebec, Canada, J1K 2R1.

0953-8984/99/030741+08$19.50

The self-consistent T-matrix approximation [19–21] provides another method for studying dynamic properties of the attractive Hubbard model. This approach is based on the low-density approximation to fermion systems due to Galitskii [22], which becomes exact in the limit of vanishing density. However, the resulting system of self-consistent integral equations is not easy to solve. Analytical treatment is very difficult, although it is sometimes attempted [23,24]. The full numerical solution of the equations is required. In the previous numerical studies of the problem [25, 26] the equations were solved for imaginary times and results were then continued numerically to real times. In these papers relatively small couplings were studied and pseudogap features were found only at large momenta.

In our previous paper [27] we formulated and solved numerically the T-matrix equations for the two-dimensional attractive Hubbard model for real times, thereby avoiding the necessity for analytical continuation. There, we focused on two-particle properties—primarily on the binding energy of pairs and its dependence on the particle density. In this paper we would like to discuss single-particle dynamics, in particular the single-particle spectral function which is directly related to angle-resolved photoemission spectra (ARPES). We find a clear pseudogap behaviour of the ARPES at small momenta $\boldsymbol{k}$, low densities n, and low temperatures T. With increasing n and T, the pseudogap disappears, in accordance with experimental observations for the cuprates [28].

The two-dimensional attractive Hubbard model is defined by the Hamiltonian

$$H = \sum_{k\sigma}(\varepsilon_{\boldsymbol{k}} - \mu)c^{\dagger}_{k\sigma}c_{k\sigma} - \frac{|U|}{N}\sum_{kpq} c^{\dagger}_{k\uparrow}c_{k+q\uparrow}c^{\dagger}_{p\downarrow}c_{p-q\downarrow} \tag{1}$$

written in standard notation. $\varepsilon_{\boldsymbol{k}} = -2t(\cos k_x + \cos k_y)$ is the bare single-particle spectrum, $|U|$ is the coupling strength, and N is the total number of sites in the system. The chemical potential μ determines the average particle density n. We regard equation (1) as a phenomenological model for the low-density system of *holes* in the normal states of HTSC.

In the low-density limit $n \ll 1$, one can make use of the small gas parameter and select only ladder diagrams in a diagrammatic representation of the T-matrix [20, 21], which leads to the expression

$$T(\boldsymbol{q},\omega) = -|U| \Big/ \left(1 - |U|\int \frac{\mathrm{d}\omega_1}{2\pi}\,\frac{B(\boldsymbol{q},\omega_1)}{\omega-\omega_1} + \mathrm{i}\frac{|U|}{2}B(\boldsymbol{q},\omega)\right) \tag{2}$$

where

$$B(\boldsymbol{q},\omega) = \frac{-1}{N}\sum_{k'}\int \frac{\mathrm{d}\omega_1}{2\pi}\,A(\boldsymbol{k}',\omega_1)A(\boldsymbol{q}-\boldsymbol{k}',\omega-\omega_1)\tanh\frac{\beta\omega_1}{2} \tag{3}$$

where $A(\boldsymbol{k},\omega)$ is the single-particle spectral function and $\beta = (k_B T)^{-1}$ is the inverse absolute temperature. The real and imaginary parts of the self-energy Σ' and Σ'' are expressed via $T = T' + \mathrm{i}T''$ as follows:

$$\Sigma'(\boldsymbol{k},\omega) = \frac{1}{N}\sum_{q}\int \frac{\mathrm{d}\omega_1}{2\pi}\,A(\boldsymbol{q}-\boldsymbol{k},\omega_1) \times \left[f_F(\omega_1)T'(\boldsymbol{q},\omega+\omega_1) + \int \frac{\mathrm{d}\omega_2}{\pi}\,\frac{f_B(\omega_2)T''(\boldsymbol{q},\omega_2)}{\omega_2-\omega_1-\omega}\right] \tag{4}$$

$$\Sigma''(\boldsymbol{k},\omega) = \frac{1}{N}\sum_{q}\int \frac{\mathrm{d}\omega_1}{2\pi}\,A(\boldsymbol{q}-\boldsymbol{k},\omega_1)T''(\boldsymbol{q},\omega+\omega_1)\,[f_F(\omega_1) + f_B(\omega+\omega_1)] \tag{5}$$

where $f_{F,B}(\omega) = [\exp(\beta\omega) \pm 1]^{-1}$ are Fermi and Bose functions respectively. Finally, the self-energy determines the spectral function as

$$A(\boldsymbol{k},\omega) = \frac{-2\Sigma''(\boldsymbol{k},\omega)}{[\omega - (\varepsilon_{\boldsymbol{k}}-\mu) - \Sigma'(\boldsymbol{k},\omega)]^2 + [\Sigma''(\boldsymbol{k},\omega)]^2}. \tag{6}$$

The integrals with singular kernels in equations (2) and (4) are understood in the principal-value sense. The set of equations (2)–(6) is to be solved self-consistently for given $|U|$, μ, and temperature T; then the particle density is given by

$$n = \frac{2}{N}\sum_{\boldsymbol{k}}\int \frac{\mathrm{d}\omega}{2\pi}\, A(\boldsymbol{k},\omega) f_F(\omega).$$

Usually, a self-consistent solution is obtained iteratively, starting from a guessed form of $A(\boldsymbol{k},\omega)$ and using the fast-Fourier-transform algorithm to calculate momentum–frequency sums [25, 26]. In our calculations we used a 64×64 lattice and a uniform mesh of 512 points in the frequency interval $-20t < \omega < 30t$. The convergence of the iterative process is the major problem of the method, which puts limitations on the values of model parameters for which a self-consistent solution can be obtained. The convergence deteriorates for large $|U|$ and n and low T. The physically interesting values of $|U|$ start at $\sim 6t$, when the binding energy of the pairs is of the order of t. In this work, $|U| = 8t$ is used. For this coupling, iterations converge down to $T = 0.3t$ for very low densities $n < 0.03$, and up to $n \sim 0.20$ for a high temperature $T = 1.0t$.

Once a self-consistent solution is obtained, the intensity of the photoemission process is simply

$$I(\boldsymbol{k},\omega) = I_0(\boldsymbol{k}) A(\boldsymbol{k},\omega) f_F(\omega) \tag{7}$$

where $I_0(\boldsymbol{k})$ involves the electron–photon matrix element, and is frequency independent. Equation (7) is approximate; for a discussion of its validity, see, e.g., [29]. In the following, we set $I_0(\boldsymbol{k}) = 1$.

In analysing the numerical results to be presented below, it is useful to keep in mind the exactly solvable atomic limit ($t = 0$) of the Hubbard model:

$$\frac{1}{2\pi} A(\boldsymbol{k},\omega) = \frac{n}{2}\delta(\omega + \mu + |U|) + \left(1 - \frac{n}{2}\right)\delta(\omega + \mu) \tag{8}$$

from which the following properties are inferred.

(a) The spectral function has the form of two peaks with weights $n/2$ and $1 - n/2$ (which are very different if $n \ll 1$).
(b) The two peaks are separated by the binding energy of the pairs (which is $|U|$ in the atomic limit).
(c) At zero temperature, $\mu = -|U|/2$, and in equation (7) the Fermi function eliminates the second peak of $A(\boldsymbol{k},\omega)$. The resulting intensity $I(\boldsymbol{k},\omega)$ is a single peak located $|U|/2$ below the chemical potential. The system would therefore display a 'pseudogap' (a true gap in this case) of size $|U|/2$.
(d) At higher temperatures, the Fermi function is smoothed out, giving rise to the second peak at a higher energy and weakening the first one, so the former might become stronger than the latter.

In the general case of finite $t/|U|$, non-zero kinetic energy leads to a number of new effects. It reduces the binding energy, i.e. the interpeak distance, and assigns finite widths to the peaks of $A(\boldsymbol{k},\omega)$. Next, it restores the $\boldsymbol{k}$-dependence of $A(\boldsymbol{k},\omega)$ and $I(\boldsymbol{k},\omega)$. Finally, due to the finite radii of pairs and their overlapping, the binding energy becomes density dependent [27]. However, our numerical results show that properties (a)–(d) listed above remain valid even at finite $t/|U|$. Moreover, we believe they are generic to any fermion model with attraction in the low-density limit.

In figure 1 we show the solution of equations (2)–(7) for the lowest density $n = 0.017$ and $T = 0.3t$. $I(\boldsymbol{k},\omega)$ displays a complicated $\boldsymbol{k}$- and ω-dependence which can be understood as

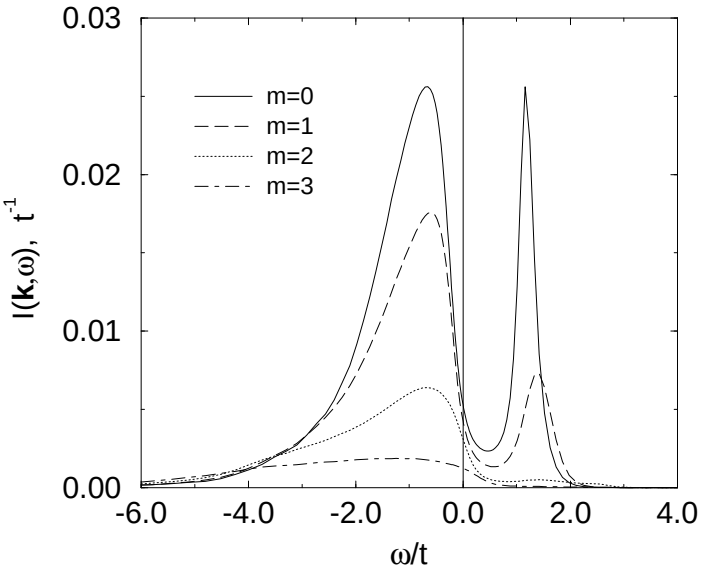

Figure 1. The intensity of the ARPES $I(\boldsymbol{k}, \omega) = A(\boldsymbol{k}, \omega) f_F(\omega)$ for density $n = 0.017$, temperature $T = 0.3t$, and several momenta $\boldsymbol{k} = m(\pi/8, \pi/8)$, $m = 0$, 1, 2, and 3 (from the top curve down).

follows. A particle with momentum $\boldsymbol{k}$ can be found in two distinctly different states: either in a state of the single-particle band with an extended wave function or as a component of a bound state with a localized wave function. The two possibilities give rise to $A(\boldsymbol{k}, \omega)$, which consists of two peaks separated by the pair binding energy $\Delta E = 2.1t$ (for $|U| = 8t$). Multiplication by the Fermi function cuts off the high-energy (single-particle band) peak, which depends on the energy of the latter and the temperature. For $\boldsymbol{k} = (0, 0)$ in figure 1, the high-energy peak is reduced in height significantly—to that of the low-energy peak, but not to zero. Note that after the cut-off, the peak is slightly shifted from its original position. The position of the high-energy peak disperses with $\boldsymbol{k}$ as does the bare spectrum $\varepsilon_{\boldsymbol{k}}$, and, as $\boldsymbol{k}$ increases, the peak gets cut off by the Fermi function very rapidly (compare the cases for the different momenta $\boldsymbol{k}$ in figure 1 for $\omega > 0$). Let us now turn to the low-energy peak. The probability of finding a particle with momentum $\boldsymbol{k}$ in a bound state is the square of the bound state's wave function. For zero total momentum $\boldsymbol{P}$, one has

$$\psi_{\boldsymbol{P}=(0,0)}(\boldsymbol{k}) = \frac{C}{E - 2\varepsilon(\boldsymbol{k})} \tag{9}$$

where C is the normalization constant and E the energy of the bound state measured from the bare atomic level. The relative height of the low-energy peaks in figure 1 is in good agreement with $|\psi(\boldsymbol{k})|^2$ for $E = 2\varepsilon(0, 0) - \Delta E = -10.1t$. This corroborates the bound-state origin of the low-energy peaks in $A(\boldsymbol{k}, \omega)$ and $I(\boldsymbol{k}, \omega)$. Thus, on the basis of figure 1, we conclude that ARPES of the attractive Hubbard model exhibit a clear pseudogap behaviour at low temperatures and densities. The momentum and frequency dependences of the spectra have simple physical explanations.

The temperature dependence of $I(\boldsymbol{k}, \omega)$ for $n = 0.017$ and $\boldsymbol{k} = (0, 0)$ is shown in fig-

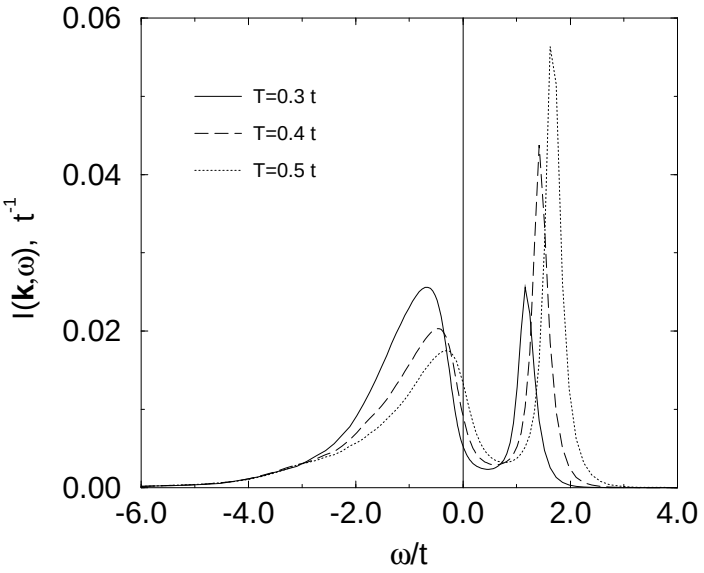

Figure 2. The temperature dependence of $I(\boldsymbol{k}, \omega)$ for density $n = 0.017$ and momentum $\boldsymbol{k} = (0, 0)$.

ure 2. There are two main effects as temperature increases. First, weight is transferred from the low-energy peak to the high-energy one. This is due to the progressive thermal excitation of particles to the single-particle band and the consequent weaker influence of the bound states on the single-particle spectral function. Secondly, the whole structure moves to higher energies relative to the chemical potential. These two effects lead to the rapid suppression of the pseudogap as temperature increases. Note that the distance between the two peaks is T-independent and remains approximately the pair binding energy (slightly reduced by the cut-off), in accordance with the atomic limit.

Figure 3 presents the density dependence of $I(\boldsymbol{k}, \omega)$ for $T = 0.5t$ and $\boldsymbol{k} = (0, 0)$. Clearly, the pseudogap disappears as n increases. We have already argued elsewhere [27] that this is a result of the rise of the two-particle level due to the packing effect when pairs begin to overlap. (Intuitive arguments of this kind were given earlier in [16].) Since the binding energy decreases with n, the temperature becomes progressively more effective in unbinding pairs, washing away the pseudogap.

It is quite remarkable that such a simple system as the attractive Hubbard model and such complex systems as high-T_c superconductors have very similar dynamical properties. They both display pseudogaps at low temperatures and carrier densities, which disappear as T and n increase. This suggests the conclusion that the carriers in HTSC do experience some sort of short-range attraction. HTSC therefore exhibit properties which are generic to fermionic systems with attraction and which are captured in our model calculations.

One could now proceed in elaborating the model while trying to keep the properties obtained intact. Further insight into the problem can be gained by considering the opposite limit of *nearly complete* filling $2 - n \ll 1$. In this case, equation (1) may be viewed as a phenomenological model for *electrons* rather than holes. (To some extent, the nearly fully

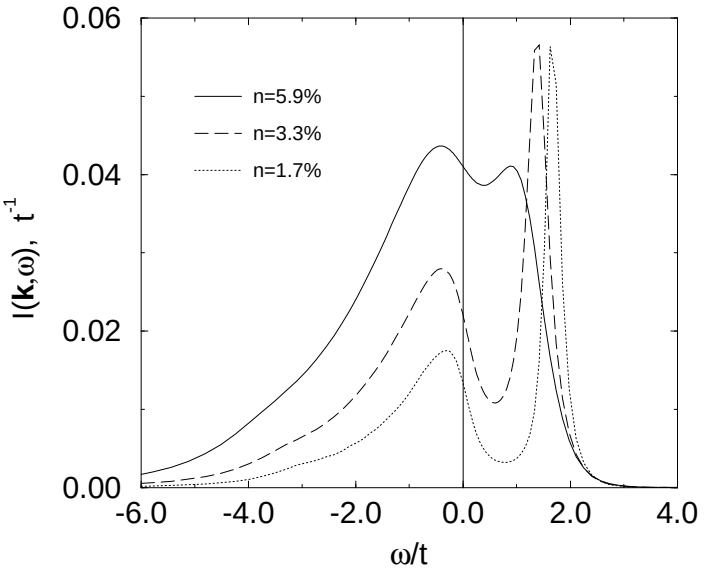

Figure 3. The density dependence of $I(\boldsymbol{k}, \omega)$ for temperature $T = 0.5t$ and momentum $\boldsymbol{k} = (0, 0)$.

filled band imitates the nearly filled lower Hubbard band when the Coulomb repulsion is taken into account. Unfortunately, this analogy is not complete, due to different temperature behaviour of μ; see below.) The quantity $I(\boldsymbol{k}, \omega)$ in equation (7) now has the meaning of the number of electrons emitted from the system per unit time, which brings the whole model closer to reality. There is no need to recalculate the spectra, since on a bipartite lattice the dilute and nearly filled limits are related by the particle–hole transformation, which leads to the relation

$$A(\boldsymbol{k}, \omega; n) f_F(\omega) = A(\boldsymbol{k} + \boldsymbol{Q}, -\omega; 2 - n)[1 - f_F(-\omega)] \tag{10}$$

where $\boldsymbol{Q} = (\pi, \pi)$ for the square lattice. Due to the inversion of the occupation numbers, it is now the pairing-induced peak that gets cut off by the Fermi function. The inversion of the frequency places the remaining peak below the chemical potential. The resulting ARPES are shown in figure 4. They are complementary to the spectra of figure 1. Clearly, a pseudogap is present, because the spectrum with the largest momentum $\boldsymbol{k} = (\pi, \pi)$ is still peaked far below the chemical potential.

The overall picture looks very much like the spectra of a weakly interacting system *but shifted* from μ by half of the pair binding energy. We emphasize that pairs themselves are *not* seen explicitly in the spectra, since the pair-induced peak of $A(\boldsymbol{k}, \omega)$ has been cut off by the Fermi function. Nevertheless, the pairs are present implicitly, manifesting themselves in the shift of the chemical potential. This observation is important for understanding the ARPES of HTSC.

We do not present temperature and density dependences of $I(\boldsymbol{k}, \omega)$ for the nearly filled case, for they are complementary to figures 2 and 3, respectively. The pseudogap now vanishes with *decreasing* electron density (increasing hole doping), in accordance with figure 3. The

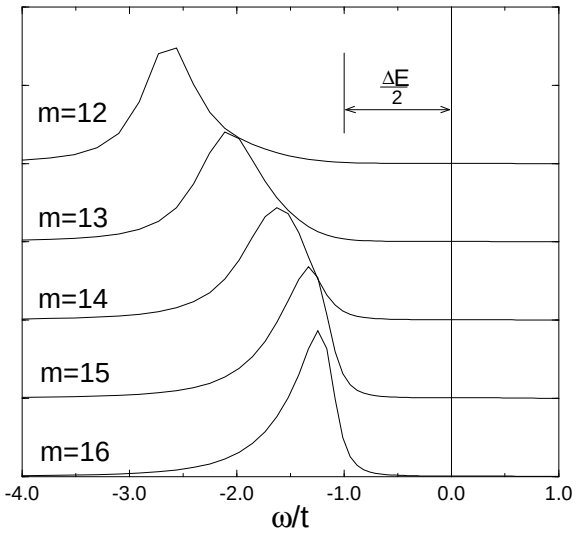

Figure 4. $I(\boldsymbol{k}, \omega)$ for nearly complete filling $n = 1.983$, temperature $T = 0.3t$, and several momenta $\boldsymbol{k} = m(\pi/16, \pi/16)$.

temperature dependence is, however, different from the dilute limit. At nearly full filling, the chemical potential *goes up* with temperature, and the distance between μ and the single-particle band increases. Therefore, the pseudogap is expected to rise with T in this case. To obtain the correct temperature behaviour, one would need to consider the density regime close to half-filling, which is outside the range of validity of the T-matrix approximation.

In conclusion, we have shown that photoemission spectra of the attractive Hubbard model in the low-density limit display a clear pseudogap behaviour, qualitatively similar to that of high-T_c superconductors. Our findings support the suggestion that the pseudogap feature observed in HTSC results from real-space pairing and the formation of bound pairs in the normal state.

Acknowledgments

We thank E G Klepfish for valuable discussions on the subject. PEK acknowledges the support of EPSRC grant GR/L40113.

References

[1] Alexandrov A S and Mott N F 1994 *High-Temperature Superconductors and other Superfluids* (London: Taylor and Francis)
[2] Takigawa M, Reyes A P, Thompson J D, Heffner R H, Fisk Z and Ott K C 1991 *Phys. Rev.* B **43** 247
[3] Williams G W M, Tallon J L, Meinhold R and Janossy A 1995 *Phys. Rev.* B **51** 16 503
[4] Loram J W, Mirza K A, Cooper J R and Liang W Y 1993 *Phys. Rev. Lett.* **71** 1740
Loram J W, Mirza K A, Wade J M, Cooper J R and Liang W Y 1994 *Physica* C **235–240** 134
[5] Ito T, Takenaka K and Uchida S 1993 *Phys. Rev. Lett.* **70** 3995
[6] Batlogg B, Hwang H Y, Takagi H, Cava R J, Kao H L and Kwo J 1994 *Physica* C **235–240** 130

[7] Rotter L D, Schlesinger Z, Collins R T, Holtzberg F, Field C, Welp U W, Crabtree G W, Liu J Z, Fang Y, Vandervoort K G and Fleshler S 1991 *Phys. Rev. Lett.* **67** 2741
[8] Homes C C, Timusk T, Liang R, Bonn D A and Hardy W N 1993 *Phys. Rev. Lett.* **71** 1645
[9] Loeser A G, Shen Z X, Dessau D S, Marshall D S, Park C H, Fournier P and Kapitulnik A 1996 *Science* **273** 325
[10] Nemetschek R, Opel M, Hoffmann C, Muller P F, Hackl R, Berger H, Forro L, Erb A and Walker E 1997 *Phys. Rev. Lett.* **78** 4837
[11] Tjernberg O, Nylen H, Chiaia G, Soderholm S, Karlsson U O, Qvarford M, Lindau I, Puglia C, Martensson N and Leonyuk L 1997 *Phys. Rev. Lett.* **79** 499
[12] Williams G V M, Tallon J L, Haines E M, Michalak R and Dupree R 1997 *Phys. Rev. Lett.* **78** 721
[13] Puchkov A V, Fournier P, Basov D N, Timusk T, Kapitulnik A and Kolesnikov N N 1996 *Phys. Rev. Lett.* **77** 3212
[14] Uemura Y J, Keren A, Le L P, Luke G M, Wu W D, Kubo Y, Manako T, Shimakawa Y, Subramanian M, Cobb J L and Markert J T 1993 *Nature* **364** 605
[15] Alexandrov A S and Ranninger J 1992 *Solid State Commun.* **81** 403
Alexandrov A S, Beere W H, Kabanov V V and Liang W Y 1997 *Phys. Rev. Lett.* **79** 1551
[16] Randeria M, Trivedi N, Moreo A and Scalettar R T 1992 *Phys. Rev. Lett.* **69** 2001
[17] Trivedi N and Randeria M 1995 *Phys. Rev. Lett.* **75** 312
[18] Vilk Y M, Allen S, Touchette H, Moukouri S, Chen L and Tremblay A-M S 1999 *J. Chem. Phys.* at press
[19] Kanamori J 1963 *Prog. Theor. Phys.* **30** 275
[20] Fetter A L and Walecka J D 1971 *Quantum Theory of Many-Particle Systems* (New York: McGraw-Hill)
[21] Kadanoff L P and Baym G 1962 *Quantum Statistical Mechanics* (New York: Benjamin)
[22] Galitskii V M 1958 *Sov. Phys.–JETP* **34** 104
[23] Kagan M Yu, Fresard R, Capezzali M and Beck H 1998 *Phys. Rev.* B **57** 5995
[24] Letz M and Gooding R J 1998 *J. Phys.: Condens. Matter* **10** 6931
[25] Frésard R, Glasser B and Wölfle P 1992 *J. Phys.: Condens. Matter* **4** 8565
[26] Micnas R, Pedersen M H, Schafroth S, Schneider T, Rodriguez-Nunez J J and Beck H 1995 *Phys. Rev.* B **52** 16 223
[27] Kyung Bumsoo, Klepfish E G and Kornilovitch P E 1998 *Phys. Rev. Lett.* **80** 3109
[28] Ding H, Yokoya T, Campuzano J C, Takahashi T, Randeria M, Norman M R, Mochiku T, Kadowaki K and Giapintzakis J 1996 *Nature* **382** 51
[29] Randeria M, Ding H, Campuzano J C, Bellman A, Jennings G, Yokoya T, Takahashi T, Katayamayoshida H, Mochiku T and Kadowaki K 1995 *Phys. Rev. Lett.* **74** 4951